

- [2] a) D. H. Williams, B. Bardsley, *Angew. Chem.* **1999**, *111*, 1264–1286; *Angew. Chem. Int. Ed.* **1999**, *38*, 1172–1193; b) K. C. Nicolaou, C. N. C. Boddy, S. Bräse, N. Winssinger, *Angew. Chem.* **1999**, *111*, 2230–2287; *Angew. Chem. Int. Ed.* **1999**, *38*, 2096–2152.
- [3] R. C. Yao, L. W. Crandall in *Glycopeptide Antibiotics* (Ed.: R. Nagarajan), Marcel Dekker, New York, **1994**, pp. 1–21.
- [4] a) S. J. Hammond, M. P. Williamson, D. H. Williams, L. D. Boeck, G. G. Marconi, *J. Chem. Soc. Chem. Commun.* **1982**, 344–346; b) S. J. Hammond, D. H. Williams, R. V. Nielsen, *J. Chem. Soc. Chem. Commun.* **1983**, 116–117.
- [5] A. M. A. van Wageningen, P. N. Kirkpatrick, D. H. Williams, B. R. Harris, J. K. Kershaw, N. J. Lennard, M. Jones, S. J. M. Jones, P. J. Solenberg, *Chem. Biol.* **1998**, *5*, 155–162.
- [6] a) The sequences of *oxyA*, *oxyB*, and *oxyC* have been deposited as part of the balhimycin biosynthesis gene cluster at the EMBL-GenBank under accession number Y16952; b) S. Pelzer, R. Süßmuth, D. Heckmann, J. Recktenwald, P. Huber, G. Jung, W. Wohlleben, *Antimicrob. Agents Chemother.* **1999**, 1565–1573.
- [7] S. Pelzer, W. Reichert, M. Huppert, D. Heckmann, W. Wohlleben, *J. Biotechnol.* **1997**, *56*, 115–128.
- [8] R. D. Süßmuth, S. Pelzer, G. Nicholson, T. Walk, W. Wohlleben, G. Jung, *Angew. Chem.* **1999**, *111*, 2096–2099; *Angew. Chem. Int. Ed.* **1999**, *38*, 1976–1979.
- [9] D. Bischoff, S. Pelzer, A. Hölzel, G. J. Nicholson, S. Stockert, W. Wohlleben, G. Jung, R. D. Süßmuth, *Angew. Chem.* **2001**, *113*, 1736–1739; *Angew. Chem. Int. Ed.* **2001**, *40*, 1693–1696.
- [10] The ¹H NMR signals of the C-O-D and of the D-O-E ring were assigned according to diagnostic NOE interactions given in the Supplementary Material of: D. L. Boger, S. Miyazaki, O. Loiseleur, R. T. Beres, S. L. Castle, J. H. Wu, Q. Jing, *J. Am. Chem. Soc.* **1998**, *120*, 8920–8926.
- [11] D. P. O'Brian, P. N. Kirkpatrick, S. W. O'Brian, T. Staroske, T. I. Richardson, D. A. Evans, A. Hopkinson, J. B. Spencer, D. H. Williams, *Chem. Commun.* **2000**, 103–104.
- [12] "Nucleic acid fragment and vector containing halogenase and method for the halogenation of chemical compounds": S. Pelzer, P. Huber, R. Süßmuth, J. Recktenwald, D. Heckmann, W. Wohlleben, Patent Wo 00/77182A1, **2000**.
- [13] H. C. Losey, M. W. Pecuh, Z. Cheng, U. S. Eggert, S. D. Dong, I. Pelzer, D. Kahne, C. T. Walsh, *Biochemistry* **2001**, *40*, 4745–4755.

Dimerization of Molecular Phosphorus Oxides

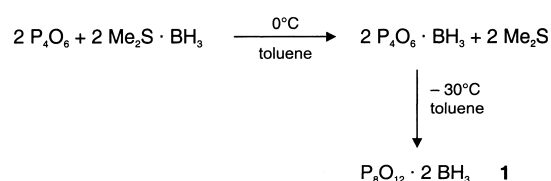
Akbar Tellenbach und Martin Jansen*

Highly symmetric, spatially closed molecular compounds are frequently much less willing to undergo reactions. Such inhibition of a reaction based on its kinetics may have considerable effects in the most diverse fields in chemistry. For instance, in chemical transport reactions involving SiF₄ as a component of the gas phase, the thermodynamically calculated transport rates are not reproduced experimentally, because the reaction back to the solid is strongly inhibited.^[1] In addition, SF₆ or CCl₄ are stable towards water at room

temperature, although in view of the thermodynamics they should undergo vigorous hydrolysis.^[2]

In this respect P₄O₆ appears particularly ambivalent, on the one hand it adds smoothly as donor ligand or reacts rapidly with water giving phosphonic acid, on the other hand it is remarkably resistant to directed ring-opening reactions. Among the few controlled and selective reactions on the adamantane-like P₄O₆ cage are the nitrene insertion^[3] and several alcoholyses.^[4] In view of this, the observation reported herein of a spontaneous dimerization of the monoborane adduct of P₄O₆ without the need for special activation was unexpected.

In the attempt to crystallize P₄O₆·BH₃,^[5,6] which forms in the stoichiometric reaction of P₄O₆ with Me₂S·BH₃, at –30 °C in a concentrated toluene solution, we obtained instead the dimer P₈O₁₂·2BH₃ (**1**) as crystalline material (Scheme 1). After three months single crystals had formed which were suitable for a crystal structure analysis.^[7]



Scheme 1. Synthesis of **1**.

The principal building block of **1** is a novel P₈O₁₂ framework, which evidently originates from the fusion of two P₄O₆ cages after cleavage of one P–O bond in each cage. As shown in Figure 1, two P₄O₆·BH₃ units were connected through two common oxygen atoms (O1, O7) in such a manner that the borane groups point in opposite directions (head–tail linkage). The dimer is folded along the two bridging oxygen atoms, resulting in dihedral angles of 151° (P1–O1–O7–P5) and 164° (P4–O7–O1–P8), respectively. The different dihedral

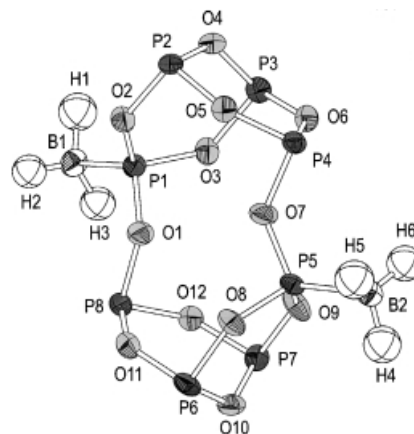


Figure 1. Molecular structure of **1** (ellipsoids for 50% probability). Selected bond lengths [pm] and angles [°]: P1–B1 187.2(2), P1–O1 158.0(2), P1–O2 158.9(2), P1–O3 158.5(2), P2–O2 166.5(2), P2–O4 163.7(2), P2–O5 162.7(2), P3–O3 166.0(2), P3–O4 163.9(2), P3–O6 162.4(2), P4–O5 162.5(2), P4–O6 163.2(2), P4–O7 165.6(2), B1–H1 113(4), B1–H2 101(3), B1–H3 119(3); O1–P1–O2 102.1(1), O1–P1–O3 103.2(1), O2–P1–O3 104.6(1), P1–O1–P8 126.8(1), P1–O2–P2 131.5(1), P1–O3–P3 135.4(1), P2–O4–P3 126.6(1), H1–B1–H2 111(3), H1–B1–H3 117(2), H2–B1–H3 118(2).

[*] Prof. Dr. M. Jansen, Dipl.-Chem. A. Tellenbach
Max-Planck-Institut für Festkörperforschung
Heisenbergstrasse 1, 70569 Stuttgart (Germany)
Fax: (+49) 711-689-1502
E-mail: martin@jansen.mpi-stuttgart.mpg.de

angles reflect an additional twisting about the O4–O10 axis, which reduces the molecular symmetry to C_1 . The P–O bond lengths vary between 157.8 and 167.1 pm and thus lie in the expected range for P–O single bonds. As in the monosubstituted P_4O_6 derivatives P_4O_7 ,^[8] P_4O_6S ,^[9] and P_4O_6Se ,^[10] starting from the four-coordinate (pentavalent) phosphorus atom an alternating shortening and lengthening of the P–O bond lengths is observed compared to those in the unsubstituted P_4O_6 molecule (P–O bond lengths 165.3 pm^[11]): Looking from P1 or P5, respectively, the first P–O bond lengths are on average 158.3, the second ones 166.3, and the subsequent ones 162.9 pm. The O–P–O bond angles vary between 95.3 and 104.7°; those at the boron-bearing phosphorus atoms tend to be larger than those at the three-coordinate phosphorus atoms. The B–P–O bond angles range between 112.5 and 118.2°, the P–O–P bond angles between 126.6 and 138.6°. The B–P bond lengths (187.2 and 186.8 pm, respectively) are somewhat shorter than those of comparable borane–phosphite adducts $(RO)_3P \cdot BH_3$ (187.9–189.5 pm;^[12] R = organic group).

The colorless crystals of **1** are stable at room temperature and inert conditions, but decompose in the presence of moist air with vigorous evolution of H_2 , and are explosive under pressure even at $-80^\circ C$. On warming to $70^\circ C$ a remarkable decomposition occurs leading to the formation of an orange-red solid, which is insoluble in toluene, above $250^\circ C$ crystalline BPO_4 (tetragonal) is formed. ^{31}P NMR spectra of **1** dissolved in toluene or CH_2Cl_2 demonstrate the immediate and complete fragmentation into two monomer units $P_4O_6 \cdot BH_3$.^[13] In the course of the dimerization one of the longest P–O bonds of the monomers is cleaved, and the resulting dangling bonds are saturated intermolecularly. Again, on dissolving the dimer, the longer P–O bonds in the asymmetric P–O–P bridges between the two $P_4O_5 \cdot BH_3$ units represent the expected point of bond cleavage.

The ^{31}P -MAS-NMR spectrum of the compound **1** is in accord with the results of the crystal structure determination, and shows a strong high-field shift for the isotropic phosphorus signals in comparison to the signals of the monomer. All eight crystallographically independent phosphorus positions are resolved in the ^{31}P -MAS-NMR spectrum (162.0 MHz, 298 K, 85 % phosphoric acid as external standard; $\delta = 66.9, 70.4, 79.0, 80.7, 81.6, 82.2, 82.8, 84.2$). Based on cross-polarization from 1H to ^{31}P spins as well as on the additional splitting through coupling to the ^{11}B nuclei, the signals at $\delta = 66.9$ and 70.4 can be assigned to the boron-bearing phosphorus atoms. As expected, the ratio between the intensities of these signals and those caused by the uncoordinated phosphorus atoms ranging from $\delta = 79.0$ to 84.2 is 2:6.

The presence of a previously unknown P_8O_{12} framework in **1** was particularly interesting in terms of the possibility of providing a route to synthesize P_8O_{12} as a new molecular phosphorus oxide through thermal or chemical abstraction of the BH_3 groups. Whereas initial preparative approaches in this direction have remained unsuccessful, we were able to detect masses in the mass spectrum of **1** at m/z 451.76 and 439.74, which correspond to $P_8O_{12} \cdot BH_3$ and to a P_4O_6 dimer, respectively; in both cases the isotopic patterns observed confirm the assignment (Figure 2).

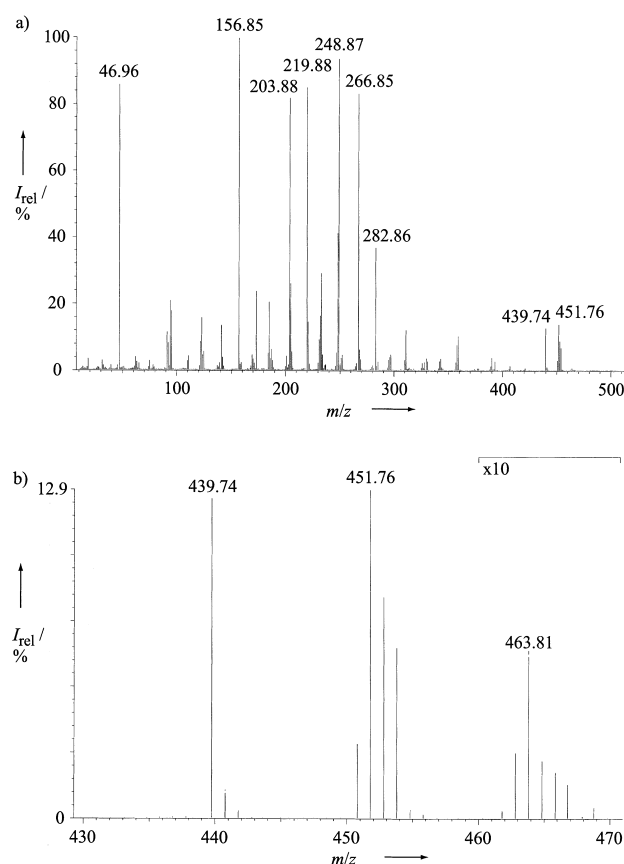


Figure 2. Mass spectrum (EI, 70 eV) of **1** at 373 K. a) Complete mass range. b) Upper mass range (from m/z 460 magnified 10-fold). m/z (%): 463.81 (0.6) [$P_8O_{12} \cdot 2BH_3^+$], 451.76 (12.9) [$P_8O_{12} \cdot BH_3^+$], 439.74 (12.6) [$P_8O_{12}^+$], 282.86 (36.6) [$P_5O_8^+$], 266.85 (83.2) [$P_5O_7^+$], 248.87 (93.7) [$P_4O_7 \cdot BH_2^+$], 219.88 (85.1) [$P_4O_6^+$], 203.88 (82.0) [$P_4O_5^+$], 156.85 (100) [$P_3O_4^+$], 46.96 (86.0) [PO^+].

The discovery of the dimerization of P_4O_6 now offers the opportunity to interpret conclusively previously not understood XANES measurements on compounds such as P_4O_7 , P_4O_6S , and P_4O_6Se . At that time, unexplicable fundamental and reversible changes of the spectra were recorded in the gas phase as a function of the temperature. In each case the spectrum calculated for the isolated molecule was only obtained at higher temperatures.^[14] By CI mass spectra of P_4O_7 we have now been able to prove that this effect is associated with a dimerization, P_4O_7 exists partially (12.1 % of the base peak, Figure 3) as a dimer in the gas phase at 323 K. Also, the ^{31}P NMR spectrum of a saturated toluene solution of P_4O_7 shows, in addition to the signals of monomeric P_4O_7 molecules, signals of weak intensity, whose relative intensity pattern, complicated multiplet structures, and chemical shifts comparable to those of **1**, suggest analogous P_4O_7 dimers.^[15]

The synthesis of **1** provides the first example of a selective linkage of molecular phosphorus oxides leading to the formation of a previously unknown P_8O_{12} framework. The dimerization detected for $P_4O_6 \cdot BH_3$ and P_4O_7 is induced by the characteristic distortion of the P_4O_6 cage caused by the attachment of a BH_3 group or an additional oxygen atom, respectively. In this process nine P–O bonds in the cage are significantly shortened, three, in contrast, lengthened. The

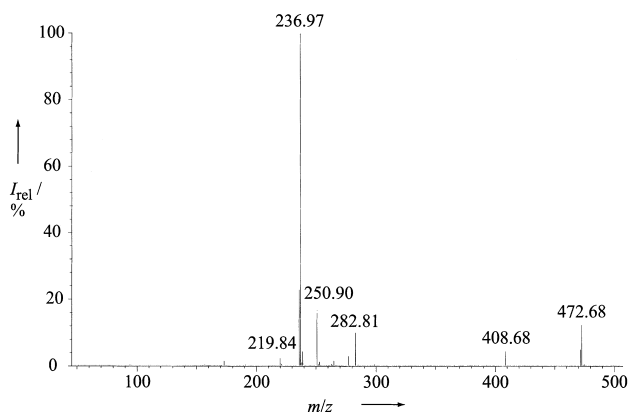


Figure 3. Mass spectrum (CI, methane) of P_4O_7 at 323 K. m/z (%): 472.68 (12.1) [$P_8O_{14}H^+$], 408.68 (4.3) [$P_7O_{12}^+$], 282.81 (9.8) [$P_5O_8^+$], 250.90 (15.7) [$P_3O_6^+$], 236.97 (100) [$P_4O_7H^+$], 219.84 (2.1) [$P_4O_6^+$].

weakening of these $P^{III}-O$ bonds as well as the shift of the electron density to the four-coordinate phosphorus atom enhances the susceptibility of the P^{III} atoms towards nucleophilic attack by oxygen atoms and explains the formation of dimers with the structure observed in **1**. The O-P-O angles in **1** are on average 100.2° and thus remain almost unchanged compared to those of the monomeric compounds P_4O_7 ,^[8] P_4O_6S ,^[9] and P_4O_6Se ^[10] (100.0°). In contrast, the average P-O-P bond angle in **1** of 132.8° is significantly larger than the corresponding value of 125.6° in the monomeric P_4O_6 derivatives, approaching the bond angles of about 140° that occur preferentially at the bridging oxygen atoms in strain-free polyphosphates and polysilicates. At the same time this widening of the angle at the oxygen atom facilitates larger P-O double-bond contributions, which is in agreement with the pronounced high-field shift of the phosphorus signals in the ^{31}P -MAS-NMR spectrum of **1** and leads to an additional stabilization of the cage. Since the number of P-O bonds remains unchanged by the dimerization, the thermodynamic driving force is predominantly considered to be the gain of additional bond enthalpy as a consequence of reduced strain in the cage, which at low temperatures evidently overcompensates the loss in entropy associated with the dimerization.

The unexpected observation of the spontaneous dimerization of molecular phosphorus oxides with an adamantane-like framework explains originally uninterpretable spectroscopic findings. Furthermore, they may help to solve other puzzling aspects of the chemistry of molecular phosphorus oxides. For example, the slow disproportionation of even highly pure P_4O_6 samples, observed on storage, could be induced by such a dimerization. The fact that the tendency to dimerize initially increases and then decreases with increasing temperature, which is confusing at first glance, can be readily understood on the basis of the interplay between the thermodynamic driving force, which favors the dimerization at low temperatures, and the kinetic inertness of the spatially closed monomers.

Experimental Section

All manipulations were carried out in glass apparatus predried under vacuum and under inert conditions (argon). P_4O_6 was distilled under

reduced pressure, toluene was heated under reflux over P_4O_{10} and freshly distilled prior to use.

$Me_2S \cdot BH_3$ (0.47 mL, 0.38 g, ca. 4.96 mmol; Strem Chemicals, in 5–6% Me_2S excess) was added dropwise under stirring to a cold solution ($0^\circ C$) of P_4O_6 (1.2 g, 5.46 mmol) in toluene (1.5 mL). The clear, colorless solution was stirred for 2 h at $0^\circ C$, and subsequently freed from Me_2S at $-10^\circ C$ under reduced pressure, until the solution stopped boiling. After storage for three months at $-30^\circ C$ the almost solidified solution was allowed to warm to room temperature; the clear, colorless crystals of **1**, which were up to 1 mm in size with a cuboid-like habit, initially remained undissolved. The crystals were separated from the mother liquor and dried under vacuum at room temperature. The powder diffractogram of the material obtained in this way was consistent with the calculated diffractogram of **1**, and showed no other additional phases.

Caution: Solid $P_8O_{12} \cdot 2BH_3$ is extremely explosive under pressure even under strict inert gas conditions and cooling to $-80^\circ C$ (friction- and shock-sensitive). We recommend that the solid is neither handled in sealed glass apparatus nor in larger amounts (maximal 1.5 g).

Received: June 1, 2001 [Z17213]

- [1] J. Hofmann, R. Gruehn, *Z. Anorg. Allg. Chem.* **1977**, 431, 105–116.
- [2] *Gmelins Handbuch der Anorganischen Chemie*, 8th ed., Schwefel, Teil B, Lieferung 3, Verlag Chemie, Weinheim, **1963**, p. 1723.
- [3] M. Jansen, S. Strojek, *J. Chem. Soc. Chem. Commun.* **1995**, 1509–1510; S. Strojek, M. Jansen, *Chem. Ber.* **1996**, 129, 121–124.
- [4] U. Schülke, *Phosphorus Sulfur Silicon* **1990**, 51/52, 153–156.
- [5] According to ^{31}P NMR spectra in solution, the previously reported,^[6] however to date not fully characterized, $P_4O_6 \cdot nBH_3$ ($n=1-3$) compounds are composed of a P_4O_6 cage with phosphorus-bound borane groups.
- [6] J. G. Riess, J. R. van Wazer, *J. Am. Chem. Soc.* **1966**, 88, 2339–2340; J. G. Riess, J. R. van Wazer, *J. Am. Chem. Soc.* **1967**, 89, 851–856; G. Kodama, H. Kondo, *J. Am. Chem. Soc.* **1966**, 88, 2045–2046.
- [7] Crystal structure analysis of **1**: SMART-1000 diffractometer with a CCD detector (Bruker AXS), crystal dimensions $0.7 \times 0.7 \times 0.7$ mm, $T=183(1)$ K, orthorhombic, space group $Pbca$ (no. 61), $a=8.606(3)$, $b=15.686(6)$, $c=22.960(9)$ Å, $V=3099(2)$ Å³, $Z=8$, $\rho_{\text{calc}}=2.003$ g cm⁻³, $2\theta_{\text{max}}=65^\circ$, $\lambda(\text{MoK}\alpha)=0.71073$ Å, ω scan, 49064 measured reflections, 5604 independent reflections, 4704 observed reflections [$I > 2\sigma(I)$], $\mu=0.952$ mm⁻¹, min./max. transmission = 0.3898/0.4991, absorption correction through symmetry-equivalent and redundant reflections (SADABS), structure solution by direct methods (SHELXS-97), structure refinement according to full-matrix least-squares procedures against F^2 (SHELXL-97), 224 parameters, hydrogen atoms refined freely (isotropic), $R_1=0.0364$, $wR_2=0.0938$ (observed reflections), min./max. residual electron density $-0.318/0.762$ e Å⁻³. Further details on the crystal structure investigation may be obtained from the Fachinformationszentrum Karlsruhe, 76344 Eggenstein-Leopoldshafen, Germany (fax: (+49)7247-808-666; e-mail: crysdata@fiz-karlsruhe.de), on quoting the depository number CSD-411904. Lattice parameters refined from powder data ($T=298$ K): $a=8.6163(2)$, $b=15.6350(3)$, $c=22.9882(5)$ Å, $V=3096.8(1)$ Å³.
- [8] M. Möbs, M. Jansen, *Z. Anorg. Allg. Chem.* **1984**, 514, 39–48; M. Jansen, M. Voss, *Angew. Chem.* **1981**, 93, 120–121; *Angew. Chem. Int. Ed. Engl.* **1981**, 20, 100; K. H. Jost, M. Schneider, *Acta Crystallogr. Sect. B* **1981**, 37, 222–224.
- [9] F. Frick, M. Jansen, P. J. Bruna, S. D. Peyerimhoff, *Chem. Ber.* **1991**, 124, 1711–1714.
- [10] J. Clade, M. Jansen, B. Engels, C. M. Marian, *Z. Anorg. Allg. Chem.* **1995**, 621, 2065–2069.
- [11] M. Jansen, M. Möbs, *Inorg. Chem.* **1984**, 23, 4486–4488; M. Jansen, M. Voss, H.-J. Deiseroth, *Angew. Chem.* **1981**, 93, 1023–1024; *Angew. Chem. Int. Ed. Engl.* **1981**, 20, 965.
- [12] J. Rodgers, D. W. White, J. G. Verkade, *J. Chem. Soc. A* **1971**, 77–80; J. C. Clardy, D. S. Milbrath, J. G. Verkade, *Inorg. Chem.* **1977**, 16, 2135–2137; T. Imamoto, E. Nagato, Y. Wada, H. Masuda, K. Yamaguchi, T. Uchimar, *J. Am. Chem. Soc.* **1997**, 119, 9925–9926.

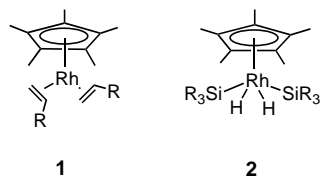
- [13] ^{31}P NMR (121.5 MHz, 298 K, 85 % phosphoric acid as external standard): $\delta = 117.1$ (d, $^2J(\text{P,P}) = 27.6$ Hz, q, $^3J(\text{P,B}) = 0.7$ Hz, 3 P; uncoordinated phosphorus), 90 (m, broadened through the quadrupole moment of boron, 1 P; boron-bearing phosphorus); compare reference [6].
- [14] C. Engemann, G. Kohring, A. Pantelouris, J. Hormes, S. Grimme, S. D. Peyerimhoff, J. Clade, F. Frick, M. Jansen, *Chem. Phys.* **1997**, 221, 189–198; C. Engemann, Dissertation, Universität Bonn, **1997**.
- [15] ^{31}P NMR (121.5 MHz, 298 K, 85 % phosphoric acid as external standard): $\delta = 94.0$ – 94.6 (m, 4 P; P^{III} corresponding to P2, P3, P6, P7 in **1**), 79.6– 80.1 (m, 2 P; P^{III} corresponding to P4, P8 in **1**), -54.3 – -53.6 (m, 2 P; P^{V} corresponding to P1, P5 in **1**).

Dehydrocoupling of Phosphanes Catalyzed by a Rhodium(II) Complex**

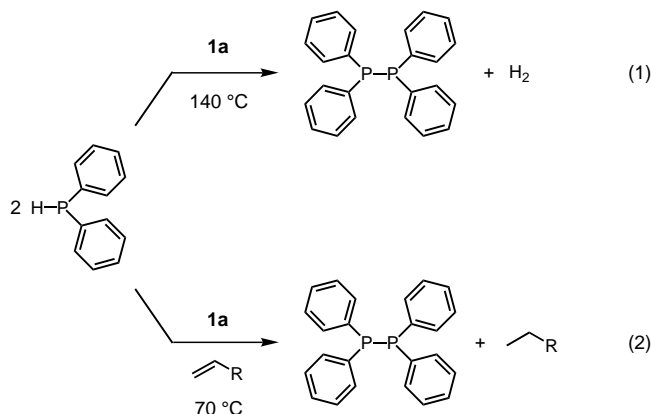
Volker P. W. Böhm and Maurice Brookhart*

Although catalytic dehydrocoupling of phosphanes has been reported with Group 4 metallocene catalysts [$\text{K}(\text{thf})_2[\text{Cp}_2^*\text{ZrH}_3]$ and $[\text{Cp}_2\text{TiMe}_2]$ ($\text{Cp}^* = \text{C}_5\text{Me}_5$, $\text{Cp} = \text{C}_5\text{H}_5$), these reactions are limited to the activation of primary phosphanes RPH_2 in the formation of (cyclic) oligomers and the cross-coupling of primary and secondary phosphanes with primary silanes.^[1–3] Late transition metal catalysis of these types of reaction has only been reported for the coupling of phosphanes with borane.^[4]

Complexes of the type $[\text{Cp}^*\text{Rh}(\text{olefin})_2]$ (**1**) are known to activate C–H bonds in arenes,^[5] olefins,^[6] aldehydes,^[7] and alkanes,^[6,8] as well as B–H bonds^[8] and such activated species have been incorporated into catalytic cycles. The rhodium(V) catalyst **2** which is a precursor to the fragment $[\text{Cp}^*\text{Rh}]$ has been used similarly for the activation of C–H bonds in arenes and alkanes as well as of Si–H bonds.^[9] Owing to the lack of reports on the activation of bonds between hydrogen and Group 15 elements, we became interested in the reactivity of secondary phosphanes towards the complex $[\text{Cp}^*\text{Rh}(\text{CH}_2=\text{CH}(\text{TMS}))_2]$ (**1a**).^[10]



Heating diphenylphosphane, HPPH_2 , in the presence of catalytic amounts of complex **1a** in C_6D_6 at 140°C results in an immediate color change of the solution from yellow to red accompanied by the formation of a new compound with a ^{31}P NMR signal at $\delta = -13.6$ which does not exhibit $^1J(\text{P,H})$ coupling. At the same time, the ^1H resonance signal for the P–H proton of HPPH_2 disappears and a signal for dihydrogen grows in at $\delta = 4.46$ [Eq. (1)]. As a side reaction, vinyltrimethylsilane is partially hydrogenated [Eq. (2)]. The product formed was identified by comparison to an authentic



sample as tetraphenyldiphosphane, Ph_4P_2 .^[11] Repeating the experiment without complex **1a** leads to the recovery of unchanged HPPH_2 . When an excess of vinyltrimethylsilane is added to the reaction, the coupling occurs at temperatures as low as 70°C and hydrogenation of the olefin is observed rather than the evolution of dihydrogen [Eq. (2)].

To investigate the scope of this catalytic reaction, various diaryl- and dialkylphosphanes were employed (Table 1). Reactivity is not sensitive to electronic effects but steric demand plays a decisive role. Mesityl (2,4,6- $\text{Me}_3\text{C}_6\text{H}_2$), *tert*-butyl, and cyclohexyl substituents prevent coupling (Table 1, entries 8, 11, and 13) whereas phenyl, *para*-anisyl, ethyl, and isobutyl groups are well-tolerated (Table 1, entries 5, 7, 9, and 10). Turnover numbers (TON) as high as 1300 mol product per mol Rh were achieved with HPPH_2 (Table 1, entry 6). An intermediate behavior is exhibited by dicyclopentylphosphane which reacts only very sluggishly (Table 1, entry 12). The rhodium catalyst **1a** also tolerates ether functionalities (Table 1, entries 7 and 17). HPPH_2 can be coupled in good yields at 110°C in the presence of vinyltrimethylsilane or 3,3-dimethyl-1-butene (Table 1, entries 1–4). Lower turnovers in comparison to those achieved in the high-temperature process without added olefin are likely due to increased formation of unreactive 18-electron species bearing olefinic ligands. No hydrophosphination of the olefin is observed in any case.^[12] Using phenylphosphane, H_2PPh , and *para*-anisylphosphane in the coupling reaction does not lead to the formation of polymeric or oligomeric polyphosphanes. Instead, the two isomers of diaryldiphosphanes, *rac*- and *meso*- ArHP-PHAr , are formed in equal amounts in low yields (Table 1, entries 14–17). Higher turnovers with primary phosphanes could be achieved only if the reaction was run in neat

[*] Prof. Dr. M. Brookhart, Dr. V. P. W. Böhm
Department of Chemistry
University of North Carolina at Chapel Hill
Chapel Hill, NC 27599-3290 (USA)
Fax: (+1) 919-962-2476
E-mail: mbrookhart@unc.edu

[**] We thank the National Institutes of Health (NIH) for financial support and O. Daugulis for samples of dimesitylphosphane and 2,4,6-tri-*tert*-butylphenylphosphane. V.P.W.B. acknowledges a Feodor Lynen fellowship of the Alexander-von-Humboldt-Stiftung (Germany).

Supporting information for this article is available on the WWW under <http://www.wiley-vch.de/home/angewandte/> or from the author.